RADIAL DISTORTION CORRECTION FROM A SINGLE IMAGE OF A PLANAR CALIBRATION PATTERN USING CONVEX OPTIMIZATION

Xianghua Ying, Xiang Mei, Sen Yang, Ganwen Wang, and Hongbin Zha

Key Laboratory of Machine Perception (Ministry of Education)
School of Electronic Engineering and Computer Science, Center for Information Science
Peking University, Beijing 100871, P.R. China

ABSTRACT

In Hartley-Kang's paper [7], they directly treated a planar calibration pattern as an image to construct an image pair together with a radial distorted image of the planar calibration pattern, and then proposed a very efficient method to determine the center of radial distortion by estimating the epipole in the radial distorted image. After determined the center of radial distortion, a least square method was utilized to recover the radial distortion function using the monotonicity constraints. In this paper, we present a convex optimization method to recover the radial distortion function using the same constraints as those required by Hartley-Kang's method, whereas our method can obtain better results of radial distortion correction. The experiments validate our approach.

Index Terms— Radial distortion, distortion correction, convex optimization, camera calibration

1. INTRODUCTION

The ideal pinhole model is often employed in algorithms of 3D recovery from 2D images in the field of computer vision. Unfortunately, for common commercially available cameras, they usually do not strictly satisfy the ideal pinhole model, i.e., some deviations may exist. Such deviations can be more complex, and are called lens distortions in literature [2]. There are many methods to model lens distortions. The most famous model was proposed by Brown [2] which described the radial, decentring and prism distortions.

In fact, among these distortions, radial distortion is the most significant in recent cameras [14], [13], [7], [12], [9], [10], [8]. Other types of distortions are often little, and can be omitted in the calibration procedure of distortion correction. Some models were proposed for the radial distortion functions. Basu and Licardie [1] proposed the logarithmic distortion model. Devernay and Faugeras [4] presented the field-of-view distortion model. Fitzgibbon [5] recommended the division model with a single parameter. Ying and Hu [13] extended the unified imaging model of central catadioptric cameras to describe the radial distortion. Hartley and Kang [7] proposed the nonparametric model. Claus and Fitzgibbon [3] constructed the rational function distortion model for a wide range of radial distortions.

In this paper, we just employ the same input image and the same constraints as required in Hartley-Kang's paper [7] for radial distortion correction using planar calibration pattern. The input image is a radial distorted image of a planar calibration pattern. The constraints are the monotonicity constraints of the radial distortion function. The main difference between [7] and ours is that we utilize a convex optimization method to recover the radial distortion function, whereas a least square method was used in [7]. Numerical experiments illustrate that our method can obtain better results of radial distortion correction than the Hartley-Kang's method [7].

The rest of this paper is organized as follows. Section 2 introduces the notations and basic principles. Section 3 presents the convex optimization method to recover the radial distortion function using the monotonicity constraints. Section 4 provides qualitative and quantitative evaluations using synthesized and real data to demonstrate the performance of our method. Section 5 concludes this paper with discussions.

2. NOTATIONS AND BASIC PRINCIPLES

In this section, we briefly introduce the Hartley-Kang's method [7] and some notions used in this paper.

2.1. Determining the center of radial distortion

Let an 2D point in the original radial distorted image or called distorted point, denoted as $\mathbf{x}^d$. Let its corresponding distortion corrected point or called undistorted point, denoted as $\mathbf{x}^u$. Indicate the center of radial distortion as $\mathbf{e}$. Since these three points $\mathbf{x}^d$, $\mathbf{x}^u$ and $\mathbf{e}$ should be collinear, we have,

$$\mathbf{x}^{d\mathrm{T}}(\mathbf{e} \times \mathbf{x}^u) = 0$$

i.e.,

$$\mathbf{x}^{d\mathrm{T}}[\mathbf{e}]_\times \mathbf{x}^u = 0 \qquad (1)$$

where $[\mathbf{e}]_\times$ is a skew-symmetric matrix to represent cross product of vectors. Let $\mathbf{x}^c$ be a point on the planar calibration pattern, then $\mathbf{x}^c$ and its corresponding

undistorted image point $\mathbf{x}^u$ are related by a 2D homography, i.e.,

$$\mathbf{x}^u \propto \mathbf{H}\mathbf{x}^c \tag{2}$$

Substituting (2) into (1), we obtain

$$\mathbf{x}^{d\mathrm{T}}[\mathbf{e}]_\times \mathbf{H}\mathbf{x}^c = 0$$

Let

$$\mathbf{F} \propto [\mathbf{e}]_\times \mathbf{H} \tag{3}$$

we obtain the usual fundamental matrix relation

$$\mathbf{x}^{d\mathrm{T}}\mathbf{F}\mathbf{x}^c = 0$$

The center of radial distortion can be recovered as the left epipole of $\mathbf{F}$ [7].

2.2. Recovering the 2D homography and the radial distortion function

Since the distortion center $\mathbf{e}$ is recovered, we can change the origin of the image coordinate system to $\mathbf{e}$, namely, now the coordinates of $\mathbf{e}$ become $\mathbf{e} = (0,0,1)^{\mathrm{T}}$. Let

$$\mathbf{F} = \begin{bmatrix} f_{11} & f_{12} & f_{13} \\ f_{21} & f_{22} & f_{23} \\ f_{31} & f_{32} & f_{33} \end{bmatrix} \tag{4}$$

and

$$\mathbf{H} = \begin{bmatrix} h_{11} & h_{12} & h_{13} \\ h_{21} & h_{22} & h_{23} \\ h_{31} & h_{32} & h_{33} \end{bmatrix} \tag{5}$$

since

$$[\mathbf{e}]_\times = \begin{bmatrix} 0 & -1 & 0 \\ 1 & 0 & 0 \\ 0 & 0 & 0 \end{bmatrix} \tag{6}$$

from (3), (4), (5) and (6), we have,

$$\begin{bmatrix} f_{11} & f_{12} & f_{13} \\ f_{21} & f_{22} & f_{23} \\ f_{31} & f_{32} & f_{33} \end{bmatrix} \propto \begin{bmatrix} 0 & -1 & 0 \\ 1 & 0 & 0 \\ 0 & 0 & 0 \end{bmatrix} \begin{bmatrix} h_{11} & h_{12} & h_{13} \\ h_{21} & h_{22} & h_{23} \\ h_{31} & h_{32} & h_{33} \end{bmatrix} = \begin{bmatrix} -h_{21} & -h_{22} & -h_{23} \\ h_{11} & h_{12} & h_{13} \\ 0 & 0 & 0 \end{bmatrix} \tag{7}$$

Therefore $[f_{31} \;\; f_{32} \;\; f_{33}] = [0 \;\; 0 \;\; 0]$. Since $\mathbf{F}$ can be determined easily, from (7) we know that the first two rows of $\mathbf{H}$ can be determined, but the third row of $\mathbf{H}$ is still unknown. In Hartley-Kang's paper [7], they employed the least square method to recover both the third row of $\mathbf{H}$ and the radial distortion function by using the monotonicity constraints (due to lack of space, we do not introduce the method here, please refer to Section 5.3, 5.4, and 5.5 in [7] for details). In this paper, we present a convex optimization method to solve this problem, as described in details below.

3. CONVEX OPTIMIZATION BASED METHOD

Changed the origin of image coordinate system to the center of radial distortion $\mathbf{e}$, a distorted point $\mathbf{x}^d = (u^d, v^d, 1)^{\mathrm{T}}$ and its corresponding undistorted point $\mathbf{x}^u = (u^u, v^u, 1)^{\mathrm{T}}$ satisfy,

$$s\begin{bmatrix} u^u \\ v^{\mathrm{u}} \end{bmatrix} = \begin{bmatrix} u^d \\ v^d \end{bmatrix}$$

i.e.,

$$\mathbf{x}^u = \begin{bmatrix} u^u \\ v^u \\ 1 \end{bmatrix} \propto \begin{bmatrix} u^d \\ v^d \\ s \end{bmatrix} \tag{8}$$

where s is some unknown non-zero scale. Let a point on the planar pattern $\mathbf{x}^c = (x, y, 1)^{\mathrm{T}}$, from (2), (5) and (8) we have,

$$\begin{bmatrix} u^d \\ v^d \\ s \end{bmatrix} \propto \begin{bmatrix} h_{11} & h_{12} & h_{13} \\ h_{21} & h_{22} & h_{23} \\ h_{31} & h_{32} & h_{33} \end{bmatrix} \begin{bmatrix} x \\ y \\ 1 \end{bmatrix} = \begin{bmatrix} h_{11}x + h_{12}y + h_{13} \\ h_{21}x + h_{22}y + h_{23} \\ h_{31}x + h_{32}y + h_{33} \end{bmatrix}$$

From above equations, we may get three equations:

$$\begin{cases} \dfrac{u^d}{v^d} = \dfrac{h_{11}x + h_{12}y + h_{13}}{h_{21}x + h_{22}y + h_{23}} \\ \dfrac{u^d}{s} = \dfrac{h_{11}x + h_{12}y + h_{13}}{h_{31}x + h_{32}y + h_{33}} \\ \dfrac{v^d}{s} = \dfrac{h_{21}x + h_{22}y + h_{23}}{h_{31}x + h_{32}y + h_{33}} \end{cases}$$

After some manipulations, we obtain,

$$\begin{cases} u^d x h_{21} + u^d y h_{22} + u^d h_{23} - v^d x h_{11} - v^d y h_{12} - v^d h_{13} = 0 \\ s x h_{11} + s y h_{12} + s h_{13} - u^d x h_{31} - u^d y h_{32} - u^d h_{33} = 0 \\ s x h_{21} + s y h_{22} + s h_{23} - v^d x h_{31} - v^d y h_{32} - v^d h_{33} = 0 \end{cases} \tag{9}$$

Note that the first equation of (9) only provides constraint on the entries of the first two rows of $\mathbf{H}$. Therefore, if given n correspondences, we may get n equations on the entries of the first two rows of $\mathbf{H}$, i.e.,

$$\begin{bmatrix} -v_1^d \mathbf{x}_1^c & u_1^d \mathbf{x}_1^c \\ \vdots & \vdots \\ -v_n^d \mathbf{x}_n^c & u_n^d \mathbf{x}_n^c \end{bmatrix} \begin{bmatrix} h_{11} \\ h_{12} \\ h_{13} \\ h_{21} \\ h_{22} \\ h_{23} \end{bmatrix} = 0 \tag{10}$$

and a least square method can be used to recover these unknowns. Now, the entries of the third row of $\mathbf{H}$, and the non-zero scales s_i $(i = 1, \ldots, n)$ for n distorted points are still unknown. From the last two equations of (9), and after some manipulations, we may obtain,

$$\begin{bmatrix} -u_1^d\mathbf{x}_1^c & \mathbf{h}_1^{\mathrm{T}}\mathbf{x}_1^c & & \\ -v_1^d\mathbf{x}_1^c & \mathbf{h}_2^{\mathrm{T}}\mathbf{x}_1^c & & \\ \vdots & & \ddots & \\ -u_n^d\mathbf{x}_n^c & & & \mathbf{h}_1^{\mathrm{T}}\mathbf{x}_n^c \\ -v_n^d\mathbf{x}_n^c & & & \mathbf{h}_2^{\mathrm{T}}\mathbf{x}_n^c \end{bmatrix} \begin{bmatrix} h_{31} \\ h_{32} \\ h_{33} \\ s_1 \\ \vdots \\ s_n \end{bmatrix} = 0 \qquad (11)$$

where

$$\mathbf{h}_1 = [h_{11}\ \ h_{12}\ \ h_{13}]^{\mathrm{T}}$$

$$\mathbf{h}_2 = [h_{21}\ \ h_{22}\ \ h_{23}]^{\mathrm{T}}$$

Note that there exists arbitrary for the entries of the third row of **H** (see Section 5.3 in [7] for details), we cannot solve these unknowns in (11) using a least square method, and the monotonicity constraints of the radial distortion function should be required to solve such arbitrary [7], namely, the monotonicity constraints on s_i. We reorder the indices i so that $\mathbf{x}_i^d$ are in ascending order of their distance to the origin. By enforcing the monotonicity constraints, we obtain a convex optimization problem,

$$\min \|\mathbf{A}\mathbf{x}\|^2 \qquad (12)$$

$$\text{subject to } s_1 \geq s_2 \geq \cdots \geq s_n$$

$$\text{and } s_1 = 1$$

where **A** is the coefficient matrix and **x** is the unknown vector in (11). We use the constraint $s_1 = 1$ to avoid the trivial solution $\mathbf{x} = 0$, and as a byproduct, it makes image points around the center of radial distortion almost no change after distortion correction. The system (12) represents a sparse convex quadratic program since $\mathbf{A}^{\mathrm{T}}\mathbf{A}$ is positive semi-definite. The optimization of this problem can be solved easily using a modern numerical package [6], [11].

4. EXPERIMENTS

We perform a number of experiments, both simulated and real, to test the performance of the proposed algorithm.

4.1. Simulation

The simulated pinhole camera has the following parameters: $f = 500$, $u_0 = 400$ and $v_0 = 300$. The resolution of the simulated image is 800×600. We generated a planar calibration pattern with 23×23 grid. The camera is fixed. The orientation and position of the planar pattern are changed. For each image taken by pinhole camera (see Fig. 1a), radial lens distortion is imposed into it by using the division model proposed in [5] (see Fig. 1b). Gaussian noise with zero-mean and σ standard deviation is added to the distorted images of these grid points. We vary the noise level σ from 0 to 1 pixel. The estimated results of the radial distortion function are shown in Fig. 2. It is not difficult to find out that the recovered distortion curves using our method are closer to the ground truth than those estimated by the Hartley-Kang's method [7]. We applied the recovered radial distortion functions to the original image, and radial distortion corrected images are obtained by using the Hartley-Kang's method and ours as shown in Fig. 3, respectively. Note that in the Hartley-Kang's method [7], it is required about twenty images of a planar pattern taken in different orientations and positions, to obtain satisfactory results of radial distortion correction (Totally 19 checkerboard images were required as shown in Fig. 3 of [7]). However, in this paper, we illustrate that only from a single image of a planar pattern, satisfactory results can still be obtained using our method.

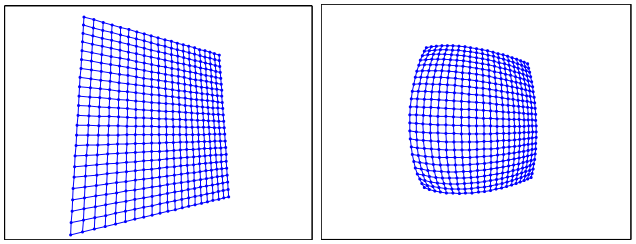

(a) (b)

Fig. 1. (a) A synthesized image of a 23×23 grid using a pinhole camera. (b) A synthesized image with radial distortion from (a).

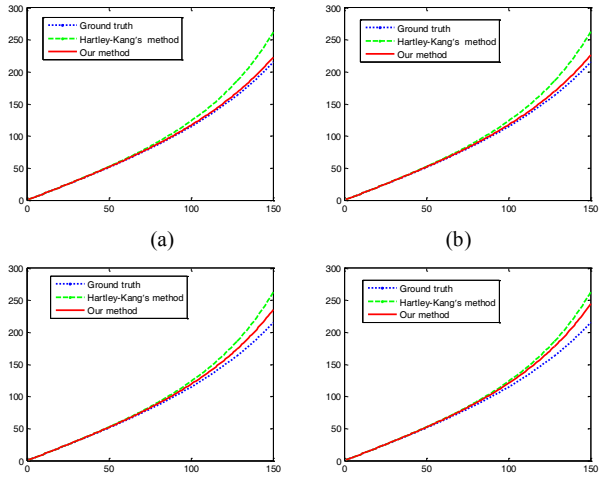

(a) (b)

(c) (d)

Fig. 2. Comparisons between algorithms of recovering radial distortion functions with respect to different noise levels. These graphs of radial distortion correction r^u versus radial position r^d are obtained by using grid points from a single image as shown in Fig. 1b. The number labels are all in pixels. (a) noise level σ = 0.25. (b) σ = 0.5 (c) σ = 0.75. (d) σ = 1.

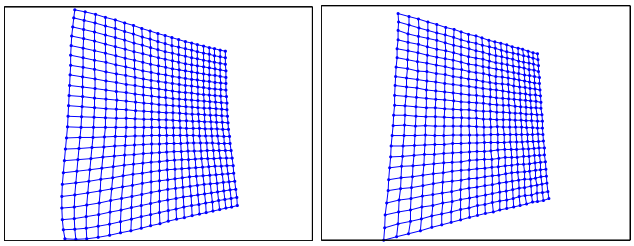

(a) (b)

Fig. 3. Results of radial distortion correction from a single image as shown in Fig1b. (a) Using the Hartley-Kang's method [7]. (b) Using our method.

4.2. Real data

A real image of a planar calibration pattern was taken by a Basler PIA2400-17gc Color high resolution machine vision camera with Fujinon FE185C046HA-1 Fish-Eye Lens, as shown in Fig. 4a. The resolution of the image is 800×600. The corrected image is shown in Fig. 4b. We also took some images in different scenes using the same camera as shown in Fig. 5a and Fig. 6a, and the corrected images are shown in Fig. 5b and Fig. 6b, respectively. All of these corrected images look very reasonable.

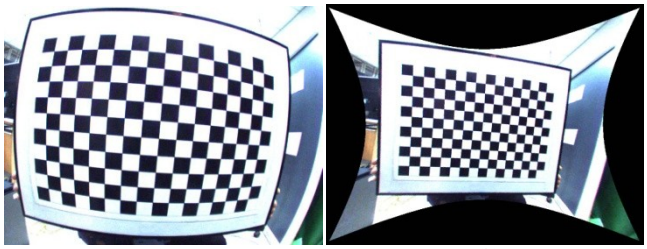

(a) (b)

Fig. 4. (a) A real image of a planar calibration pattern with radial distortion. (b) The corrected image from (a).

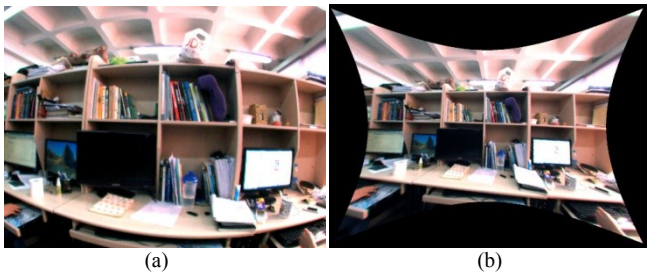

(a) (b)

Fig. 5. (a) A real image of a book shelf with radial distortion. (b) The corrected image from (a).

(a) (b)

Fig. 6. (a) A real image of a corridor with radial distortion. (b) The corrected image from (a).

5. CONCLUSIONS

This paper presents a convex optimization based method for radial lens distortion correction from a single image of a planar pattern by using the monotonicity constraints of radial distortion function. In the Hartley-Kang's method, it is required about twenty images of a planar pattern taken in different orientations and positions, to obtain satisfactory results of radial distortion correction using a least square method. However, in this paper, we illustrate that only utilizing a single radial distorted image of a planar pattern, reasonable corrected results can still be obtained by using our method, and the corrected results may be better than those from the Hartley-Kang's method in the same situation.

ACKNOWLEDGMENT

This work was supported in part by NKBPRC 973 Grant No. 2011CB302202, NNSFC Grant No. 61322309, NNSFC Grant No. 61273283, NNSFC Grant No. 91120004, and NHTRDP 863 Grant No. 2009AA01Z329.

REFERENCES

[1] A. Basu and S. Licardie, “Alternative models for fish-eye lenses,” Pattern Recognition Letters, vol. 16, no. 4, pp. 433–441, Apr. 1995.

[2] D. C. Brown, “Close-range camera calibration,” Photogrammetric Engineering, vol. 37, no. 8, pp. 855–866, 1971.

[3] D. Claus and A. Fitzgibbon, “A rational function lens distortion model for general cameras,” Proc. IEEE Int’l Conf. Computer Vision and Pattern Recognition, pp. 213–219, 2005.

[4] F. Devernay and O. Faugeras, “Straight lines have to be straight,” Machine Vision and Applications, vol. 13, no.1, pp. 14-24, 2001.

[5] A. Fitzgibbon, “Simultaneous linear estimation of multiple view geometry and lens distortion,” Proc. IEEE Int’l Conf. Computer Vision and Pattern Recognition, pp. 125–132, 2001.

[6] M. Grant, S. Boyd, Y. Ye. Disciplined Convex Programming. Global Optimization: From Theory to Implementation, Kluwer, 2005.

[7] R. Hartley and S. Kang, “Parameter-free radial distortion correction with center of distortion estimation,” IEEE Trans. Pattern Analysis and Machine Intelligence, vol. 29, no. 8, pp. 1309–1321, 2007.

[8] K. Kanatani, "Calibration of ultrawide fisheye lens cameras by eigenvalue minimization," IEEE Transactions on Pattern Analysis and Machine Intelligence, vol. 35, no. 4, pp. 813-822, 2013.

[9] Z. Kukelova and T. Pajdla, “A minimal solution to radial distortion autocalibration,” IEEE Trans. Pattern Analysis and Machine Intelligence, vol. 33, no. 12, pp. 2410-2422, 2011.

[10] Z. Kukelova, M. Bujnak and T. Pajdla, “Real-time solution to the absolute pose problem with unknown radial distortion and focal length,” Proc. Fifth IEEE Int’l Conf. Computer Vision, 2013.

[11] J.F. Sturm, “Using SeDuMi 1.02, A Matlab toolbox for optimization over symmetric cones,” Optimization Methods and Software, vol. 11-12, pp. 625-633, 1999.

[12] J. Tardif, P. Sturm, S. Roy, “Plane-based self-calibration of radial distortion,” Proc. Fifth IEEE Int’l Conf. Computer Vision, pp. 1-8, 2007.

[13] X. Ying and Z. Hu, “Can we consider central catadioptric cameras and fisheye cameras within a unified imaging model?” Proc. European Conference on Computer Vision, vol. I, pp.442-455, 2004.

[14] Z. Zhang, “Flexible camera calibration by viewing planes from unknown orientations,” Proc. Seventh Int’l Conf. Computer Vision, pp. 666-673, 1999.